5-31-1992

Local stress due to a radial loading at nozzle-pipe connection with different thickness

Guosheng Lu
New Jersey Institute of Technology

ABSTRACT

Local Stress Due to A Radial loading At Nozzle-pipe Connection with Different Thickness

by
Guosheng Lu

This thesis presents an analysis using the finite element method of the local stress at the nozzle and pipe connection subjected to a radial loading.

In this study, the local stress factor (for membrane and bending stresses) is presented in a series of plots with beta (nozzle radius/pipe radius) values ranging from 0.1 to 1.0 and gamma (pipe radius/wall thickness) values ranging from 10 to 100. The membrane and bending stresses in longitudinal and circumferential directions of the run pipe are computed as a function of the dimensionless parameters, beta and gamma.

For a given external radial loading with different nozzle and pipe wall thickness, the different bending moment and membrane stresses produced are obtained for the range of parameter values gamma and beta mentioned above. The values of beta, wall thickness and location have a significant effect on the values of the stresses. The more the ratio of nozzle wall thickness to vessel wall thickness varies from unity, the greater the stresses . The stresses decrease as beta increases.

LOCAL STRESS DUE TO A RADIAL LOADING AT NOZZLE-PIPE CONNECTION WITH DIFFERENT THICKNESS

by
Guosheng Lu

A Thesis
Submitted to the Faculty of the New Jersey Institute of Technology
in Partial Fulfillment of the Requirements for the Degree of
Master of Science
Department of Mechanical Engineering
May 1992

APPROVAL PAGE

Local Stress Due to A Radial Loading At Nozzle-pipe connection with Different Thickness

by

Guosheng Lu

Dr. Benedict C. Sun, Thesis Advisor
Associate Professor of Engineering Technology, NJIT

Dr. Bernhard Koplik
Professor of Mechanical Engineering, NJIT

Dr. Harry Herman
Professor of Mechanical Engineering, NJIT

James Miller
Associate Professor of Engineering Technology, NJIT

Dr. Rong-Yaw Chen
Professor of Mechanical Engineering, NJIT

BIOGRAPHICAL SKETCH

Author: Guosheng Lu

Degree: Master of Science in Mechanical Engineering

Date: May, 1992

Undergraduate and Graduate Education:

- Master of Science in Mechanical Engineering,
  New Jersey Institute of Technology, Newark,NJ, 1992
- Bachelor of Science in Naval Architecture and Ocean Engineering
  Shanghai Jiao Tong University, Shanghai, China, 1982

Major: Mechanical Engineering

ACKNOWLEDGEMENT

I would like to express my sincere gratitute to my advisor, Dr. Benedict C. Sun, for his guidance, friendship and moral support throughout the course of this work.

My special thanks to Professor Bernard Koplik, Professor Harry Herman, Associate Professor James Miller and Professor Rong-Yaw Chen for serving as members of the committee.

I am thankful to all my friends and family members for supporting and encouraging me to complete my work successfully.

TABLE OF CONTENTS

LIST OF TABLES

LIST OF FIGURES

Figure Page

LIST OF NOMENCLATURE

$\beta = \frac{r_n}{R_p}$, beta

$\Upsilon = \frac{R_p}{T}$, gamma

σ_i = normal stress in the ith direction on the surface of shell, psi

i = denotes direction (longitudinal and circumferential direction of the run pipe)

ϕ = circumferential direction

x = longitudinal direction

j = denotes location (on the nozzle and pipe)

n = on the nozzle

p = on the pipe

K_m = membrane stress concentration factor

K_{mn} = membrane stress concentration factor of the nozzle

K_{mp} = membrane stress concentration factor of the pipe

K_b = bending stress concentration factor of the nozzle

K_{bn}= bending stress concentration factor of the nozzle

K_{bp} = bending stress concentration factor of the pipe

l = length of pipe, in

M_x = bending moment, in longitudinal direction, in-lb/in

M_{xn} = bending moment in longitudinal direction of the nozzle, in-lb/in

M_{xp} = bending moment in longitudinal direction of the pipe, in-lb/in

M_ϕ = bending moment in circumferential direction, in-lb/in

$M_{\phi n}$ = bending moment in circumferential direction of the nozzle, in-lb/in

$M_{\phi p}$ = bending moment in circumferential direction of the pipe, in-lb/in

N_x = membrane force in longitudinal direction, lb/in

N_{xn} = membrane force in longitudinal direction of the nozzle, lb/in

N_{xp} = membrane force in longitudinal direction of the pipe, lb/in

N_ϕ = membrane force in circumferential direction, lb/in

$N_{\phi n}$ = membrane force in circumferential direction of the nozzle, lb/in

$N_{\phi p}$ = membrane force in circumferential direction of the pipe, lb/in

r_n = mean radius of nozzle, in ($r_n = \beta R_p$ in this thesis)

R_p = mean radius of pipe, in

t = wall thickness of nozzle, in (t= βT in this thesis)

T = wall thickness of pipe, in

CHAPTER I
INTRODUCTION

It is known that there exists highly localized stresses due to external loadings at the juncture of the nozzle and pipe for a nozzle-pipe connection. The local stresses along the intersecting juncture are always major concerns for designers. With the development of the computer, the local stresses due to external loadings of a nozzle-pipe connection can be accurately evaluated with sophisticated computer software such as ANSYS, using the finite element approach to describe the real geometries and loading conditions.

This thesis studies the local stresses both on the pipe and on the nozzle at a pipe-nozzle connection subjected to an external radial loading.

In this thesis, the finite element method simulates the real nozzle-pipe geometry at the juncture. A radial loading is applied uniformly downward through the nozzle onto the juncture. It is considered that the wall thickness of the nozzle is β times the wall thickness of the pipe. Due to symmetry of the pipe-nozzle connection, only one quarter of the connection is used to simulate the total geometry.

Since stresses may be different in the nozzle and the pipe, the local stresses on both the pipe and the nozzle are investigated for both points A and C (see figure 1) . At each point, there are longitudinal and circumferential stresses on the pipe and the nozzle. Each of the above stresses, is further divided into membrane and bending stresses. A total of sixteen different stresses are investigated. These stresses are normalized, by their respective geometries, i.e. stress factors that are functions of beta and gamma, Υ, (pipe radius/pipe wall thickness). β ranges from 0.1 to 1.0, and Υ ranges from 10 to 100.

CHAPTER II
THE DEVELOPMENT OF STRESS ANALYSIS ON THE NOZZLE-PIPE CONNECTION

2.1 THEORY AND EXPERIMENT

In 1955, Prof. Bijlaard [1] provided an analytical method for determining the stresses in pressure vessel nozzle connections subjected to various forms of external loadings. Bijlaard's work is based on thin-shell theory using a double Fourier series solution.

From Bijlaard 's study, K. R. Wichman, A. G. Hopper and J. L. Mershon[2] published WRC Bulletin No. 107, in 1965. It suggests a procedure to calculate the local stresses in spherical and cylindrical shells due to external loadings.

Gwaltney et al [3] in 1976, published some experimental data for cylinder-to cylinder shell models in "Experimental stress analysis of cylinder-to-cylinder shell models and comparison with the theoretical predictions."

Brown et al [4] in 1977, published "Analytical and experimental stress analysis of a cylinder-to-cylinder structure."

Early researches by either analytical or experimental method, due to the mathematical limitations on Bijlaard's solution and experimental conditions (cost, material, and instrumentation limitation), were not possible for a larger nozzle radius , namely β (nozzle radius/pipe radius) greater than 0.5.

2.2 FINITE ELEMENT METHOD

With the development of computer method, local stress on a nozzle-pipe connection can be evaluated by the finite element method with sophisticated computer programs.

Sadd and Avent [5] in 1982 studied a trunnion pipe anchor by the finite element method. The model is analyzed for the case of internal pressure and moment loadings.

Tabone and Mallett [6] in 1987 established a finite element model of a nozzle on a cylindrical shell subjected to internal pressure, out-of-plane moment, and a combination of internal pressure plus out-of-plane moment. The model used ANSYS three-dimensional finite elements and considered inelastic behavior at small displacements.

Mirza and Gupgupogu [7] in 1988 introduced 17-node doubly curved shell finite elements to simulate the case of longitudinal moments applied at discrete points around the circumference of the pipe.

Sun and Sun [8] in 1988 published the local stresses on piping-nozzle connections due to radial load, circumferential and longitudinal moments obtained by the finite element approach.

Sun and Sun [9], in 1990, extended their previous studies to the area of torsion and shear loading. Since the finite element method was used for the studies, Sun and Sun [8] [9] were able to investigate the local stresses due to large nozzle-to-pipe radius ratios. However they focused their stress studies on the pipe portion by assuming that the nozzle and pipe have the same wall thickness. That is t=T.

Questions arise concerning the local stresses on the nozzle portion of the connection. If the nozzle and pipe wall thicknesses are not under equal, would it be possible that the maximum stresses occur on the nozzle portion ? Studies by Sun & Sun and previous authors have not answered this question. It is the intent of this thesis to study the local stresses on both the pipe and nozzle separately.

CHAPTER III
BASIC EQUATION AND CALCULATION OF STRESS

With the aid of thin-shell theory, Bijlaard [1] developed analytical solutions for local stresses in cylindrical shells with loading over a rectangular area, using an eighth order partial differential equation [10]. Results from Bijlaard were arranged for tabular calculation by K. R. Wichman, A. G. Hopper and J. L. Mershon [2]. This latter work introduced stress factors that are functions of beta and gamma. This is the well-known Bulletin No.107 method.

In this thesis, the definitions for beta and gamma are retained, so that this work may complete the results for Bulletin 107.

3.1 BASIC EQUATION

In the analysis of stresses in thin shells, the numerical results show a biaxial state of stress in the circumferential and longitudinal directions. Each stress has two components, the membrane stress and bending stress. One proceeds by considering the relation between internal membrane force, internal bending moments and stress concentrations in accordance with the following:

$$\sigma_{in} = K_{mn}\frac{N_{in}}{t} \pm K_{bn}\frac{6M_{in}}{t^2} \qquad \text{(on the nozzle)}$$

$$\sigma_{ip} = K_{mp}\frac{N_{ip}}{T} \pm K_{bp}\frac{6M_{ip}}{T^2} \qquad \text{(on the pipe)}$$

Subscript i stands for either x (longitudinal direction) or ϕ (circumferential direction).

3.2 CALCULATION OF STRESS

3.2.1. Circumferential stress(σ_{ϕ})

On the nozzle
$$\frac{N_{\phi n}}{t} = \left[\frac{N_{\phi n}}{P/r_n}\right] \cdot \left[\frac{P}{r_n \cdot t}\right]$$ (membrane stress)

$$\frac{6M_{\phi n}}{t^2} = \left[\frac{M_{\phi n}}{P}\right] \cdot \left[\frac{6P}{t^2}\right]$$ (bending stress)

$$\sigma_{\phi n} = K_{mn}\frac{N_{\phi n}}{t} \pm K_{bn}\frac{6M_{\phi n}}{t^2}$$

On the pipe
$$\frac{N_{\phi p}}{T} = \left[\frac{N_{\phi p}}{P/R_p}\right] \cdot \left[\frac{P}{R_p \cdot T}\right]$$ (membrane stress)

$$\frac{6M_{\phi p}}{T^2} = \left[\frac{M_{\phi p}}{P}\right] \cdot \left[\frac{6P}{T^2}\right]$$ (bending stress)

$$\sigma_{\phi p} = K_{mp}\frac{N_{\phi p}}{T} \pm K_{bp}\frac{6M_{\phi p}}{T^2}$$

3.2.2. Longitudinal stress (σ_x)

On the nozzle
$$\frac{N_{xn}}{t} = \left[\frac{N_{xn}}{P/r_n}\right] \cdot \left[\frac{P}{r_n \cdot t}\right]$$ (membrane stress)

$$\frac{6M_{xn}}{T^2} = \left[\frac{M_{xn}}{P}\right] \cdot \left[\frac{6P}{T^2}\right]$$ (bending stress)

$$\sigma_{xn} = K_{mn}\frac{N_{xn}}{t} \pm K_{bn}\frac{6M_{xn}}{t^2}$$

On the pipe
$$\frac{N_{xp}}{T} = \left[\frac{N_{xp}}{P/R_p}\right] \cdot \left[\frac{P}{R_p \cdot T}\right]$$ (membrane stress)

$$\frac{6M_{xp}}{T^2} = \left[\frac{M_{xp}}{P}\right] \cdot \left[\frac{6P}{T^2}\right] \qquad \text{(bending stress)}$$

$$\sigma_{xp} = K_{mp}\frac{N_{xp}}{T} \pm K_{bp}\frac{6M_{xp}}{T^2}$$

All calculation of stresses are summarized in Table 1 and Table 2. The stress direction is as shown in Figure 1

.

Table 1: Computation sheet for local stresses on the nozzle

Figure	Stress factor	Stress component	Stress direction
Nozzle2-3 Nozzle1-4	$\frac{N_{\phi n}}{P/r_n}$	$K_{mn}\left[\frac{N_{\phi n}}{P/r_n}\right] \cdot \frac{P}{r_n \cdot t}$	ϕ
Nozzle2-2 Nozzle1-1	$\frac{M_{\phi n}}{P}$	$K_{bn}\left[\frac{M_{\phi n}}{P}\right] \cdot \frac{6P}{t^2}$	ϕ
Nozzle2-4 Nozzle1-3	$\frac{N_{xn}}{P/r_n}$	$K_{mn}\left[\frac{N_{xn}}{P/r_n}\right] \cdot \frac{P}{r_n \cdot t}$	x
Nozzle2-1 Nozzle1-2	$\frac{M_{xn}}{P}$	$K_{bn}\left[\frac{M_{xn}}{P}\right] \cdot \frac{6P}{t^2}$	x

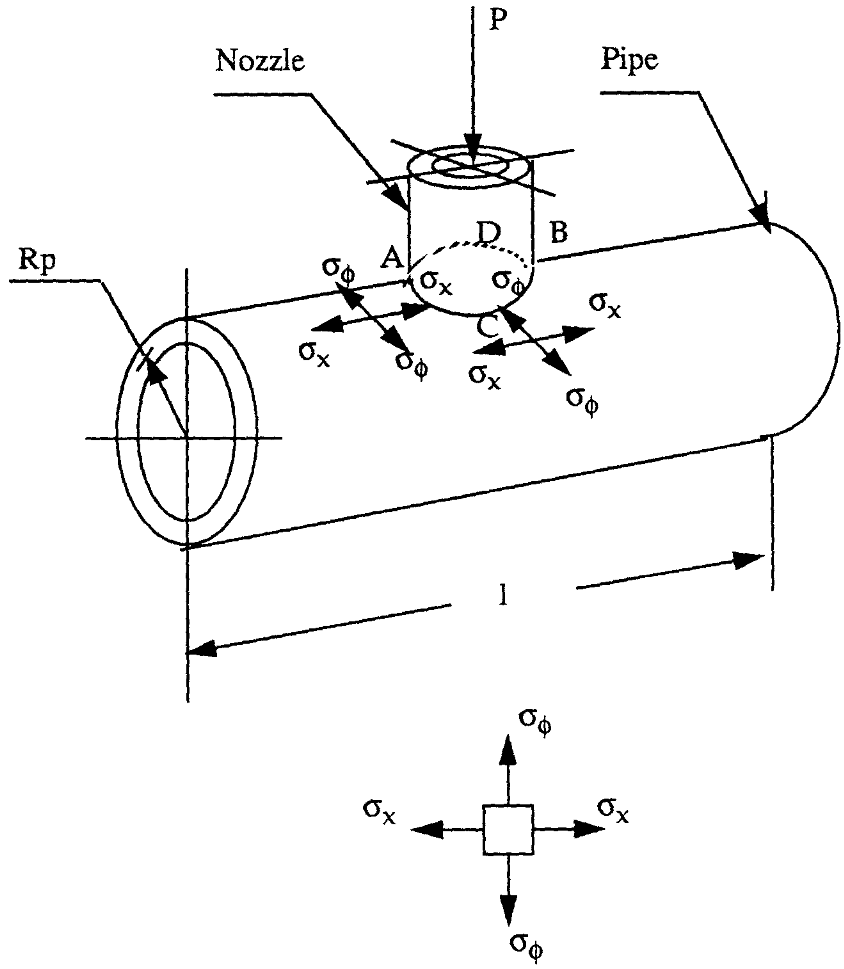

Figure 1. Typical configuration of nozzle-pipe connection for an external radial loading and stress direction

Table 2: Computation sheet for local stresses on the pipe

Figure	Stress factor	Stress component	Stress direction
Pipe2-3 Pipe1-4	$\frac{N_{\phi p}}{P/R_p}$	$K_{mp}\left[\frac{N_{\phi p}}{P/R_p}\right]\cdot\frac{P}{R_p\cdot T}$	ϕ

Table 2: Computation sheet for local stresses on the pipe

Figure	Stress factor	Stress component	Stress direction
Pipe2-2 Pipe1-1	$\frac{M_{\phi p}}{P}$	$K_{bp}\left[\frac{M_{\phi p}}{P}\right]\cdot\frac{6P}{T^2}$	ϕ
Pipe2-4 Pipe1-3	$\frac{N_{xp}}{P/R_p}$	$K_{mp}\left[\frac{N_{xp}}{P/R_p}\right]\cdot\frac{P}{R_p\cdot T}$	x
Pipe2-1 Pipe1-2	$\frac{M_{xp}}{P}$	$K_{bp}\left[\frac{M_{xp}}{P}\right]\cdot\frac{6P}{T^2}$	x

3.3 SIGN CONVENTION

Sign convention on the nozzle, different from that on the pipe, is discussed in the following:

3.3.1. Sign convention on the pipe

The radial local P acts from nozzle to pipe inward causing compressive membrane stresses. Furthermore, local bending occur so that tensile bending stresses result on the inside wall of the pipe i.e. A_l, B_l, C_l, D_l while compressive bending stresses result on the outside wall i.e. A_u, B_u, C_u, and D_u. (Figure 2).

3.3.2. Sign convention on the nozzle

An external radial loading P acts similarly to a local external pressure on the nozzle causing compressive membrane stresses and bending stresses on both sides of the vessel at E, F, G, H, (E, F, G, H are located on the nozzle) in Figure 3.

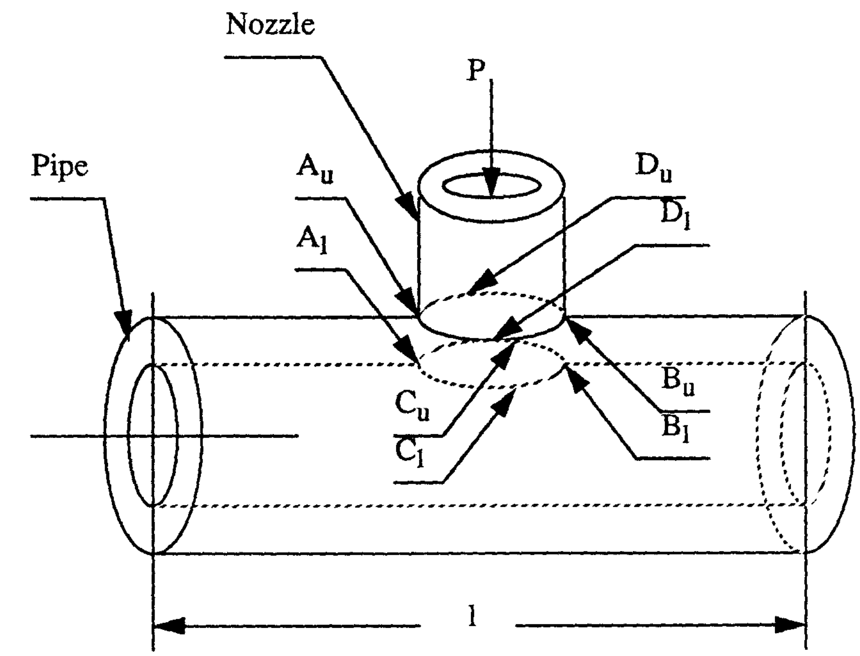

Figure 2. Stress location on the pipe

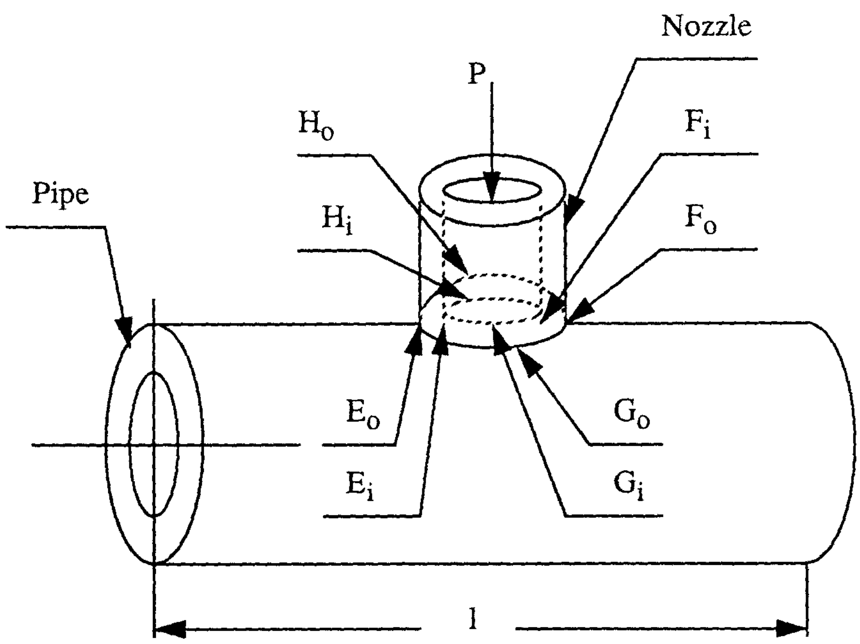

Figure 3. Stress location on the nozzle

Sign notations on the pipe and the nozzle are summarized in Table 3. and Table 4.

Table 3: Sign Convention on the Pipe for Stresses Resulting from a Radial Loading

Stress	Location	Sign convention
Membrane stress	A_u, A_l	-
$\frac{N_{xp}}{T}$ and $\frac{N_{\phi p}}{T}$	B_u, B_l	-
	C_u, C_l	-
	D_u, D_l	-
Bending stress	A_u, B_u	-
$\frac{6M_{xp}}{T^2}$ and $\frac{6M_{\phi p}}{T^2}$	C_u, D_u	-
	A_l, B_l	+
	C_l, D_l	+

u----- upper surface of the pipe   l-------low surface of the pipe

Table 4: Sign Convention on the Nozzle for Stresses Resulting from a Radial Loading

Stress	Location	Sign convention
Membrane stress	E_o, E_i	-
$\frac{N_{xn}}{t}$ and $\frac{N_{\phi n}}{t}$	F_o, F_i	-
	G_o, G_i	-
	H_o, H_i	-
Bending stress	E_o, E_i	-
$\frac{6M_{xn}}{t^2}$ and $\frac{6M_{\phi n}}{t^2}$	F_o, F_i	-
	G_o, G_i	-
	H_o, H_i	-

o------outside surface of the nozzle   i-------inside surface of the nozzle

CHAPTER IV
FINITE ELEMENT MODEL

In this thesis, by using the ANSYS general finite element program from Swanson Analysis Systems, Inc [11], the nozzle-pipe connection is modeled by using quadrilateral thin shell element (STIF 63, thin shell element), for wide ranges of beta and gamma.

4.1 ASSUMPTION OF MODEL

For the analysis of this model, the following assumptions are used.thus

A. The material is assumed to be homogeneous, and in the elastic range, it obeys Hooke's Law. The resulting stresses and strains are within the proportional limit of the material.

B. The internal pressure is not taken into account.

C. The influences of materialf-weight and temperature are neglected.

D. There are no transitions, fillets, or reinforcing at the juncture.

E. The pipe is so long that its end conditions have no significant effect on the local stresses.

4.2 PARAMETERS

The results of this work have been plotted in terms of nondimensional geometric parameters. Hence, the first step is to evaluate the applicable geometric parameters.

4.2.1. Pipe parameter (Υ)

The pipe parameter is given by the ratio of the pipe mean radius to pipe thickness thus:

$$\Upsilon = \frac{R_p}{T}$$

4.2.2. Nozzle parameter (β)

The nozzle parameter β is evaluted by the ratio of the nozzle mean radius to pipe mean radius

$$\beta = \frac{r_n}{R_p}$$

4.2.3. Length of pipe (l)

The length of pipe is assumed to be at least 8 times the pipe mean radius

$$l \geq 8 \cdot R_p$$

4.2.4. The thickness of nozzle (t)

The wall thickness of the nozzle(t) is taken as β times the wall thickness of the pipe (T), i.e.

$$t = \beta T$$

4.2.5. The relation of radius between the nozzle and pipe

The relation of radius between the nozzle and pipe is as follow:

$$r_n = \beta Rp$$

4.3 ESTABLISHMENT OF MODEL

Since the geometry of the model, elastic properties, and support conditions are symmetric with respect to the x-y plane and y-z planes, only one quarter of the geometry is necessary if a loading applied to the model is symmetric or uniformly distributed. Hence, a quarter portion of the geometry is used (Figure 4) as the computational model by setting constraints along the planes of symmetry.

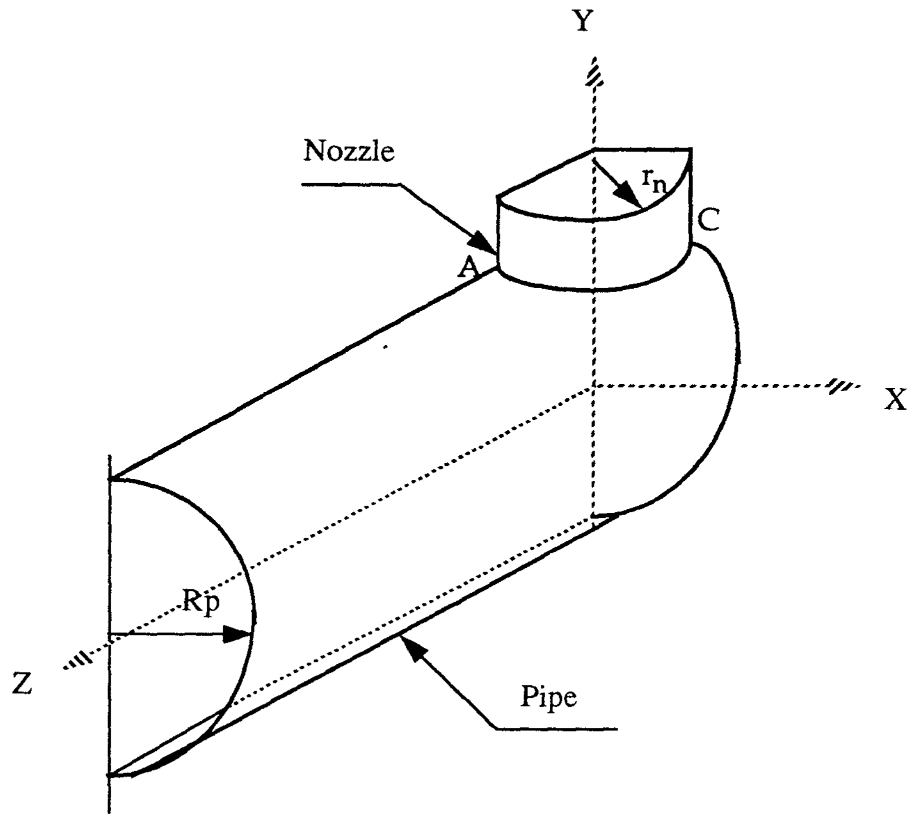

Figure 4. A quarter model of the nozzle-pipe juncture

4.3.1. Boundary condition

Since the radial force is applied from the top of the nozzle, the radial force is uniformly distributed in the negative y direction . The geometry of the structure and the applied loading are symmetric with respect to the x-y and y-z planes, therefore the displacement in the z direction for all nodes on the x-y plane and the displacement in the x direction for all nodes on the y-z plane are restrained. Correspondingly, rotations around the x-axis and the y-axis for all nodes on the x-y plane and rotations around the y-axis and z-axis for all nodes on the y-z plane are restrained.

4.3.2. Element model

In the ANSYS finite element package, the subroutine called PREP 7 is used to generate the geometry. First, we define 17 keypoints to divide the model into 9 areas, A1 and A2 are generated with one cylidrical coordinate system and A3 to A9 are generated with another cylindrical coordinate system. (Figure 5). Element type STIF 63 is used to generate the model which is a quadrilateral in shape with one node at each corner.

4.3.3. Loading condition

In a quadrilateral thin shell element model, there are 25 nodes (24 elements) on the nozzle opening. In studying the radial loading case, the radial force is distributed equally at those nodes except for two nodes located on the planes of symmetry at each end. At thses two points the values of the model force should be half of the value elsewhere to satisfy the symmetry condition. In the actual computation, an external radial loading of 1000 pounds is applied at the top of the entire nozzle, which is equivalent to a 250 pounds force applied to the quarter model. Therefore, each node supports 10.416667 pounds of nodal force in the negative y direction,and the node at each ends support 5.208333 pounds.

4.3.4. Results

Using the finite element method, from the ANSYS program, the stress results are resolved into membrane stresses and bending stresses at points A and C on the pipe and at points E and G on the nozzle. Then the stresses are translated into stress factors; there are four different stress fators for each of the points A, C, E, and G as summarized in Table 5.

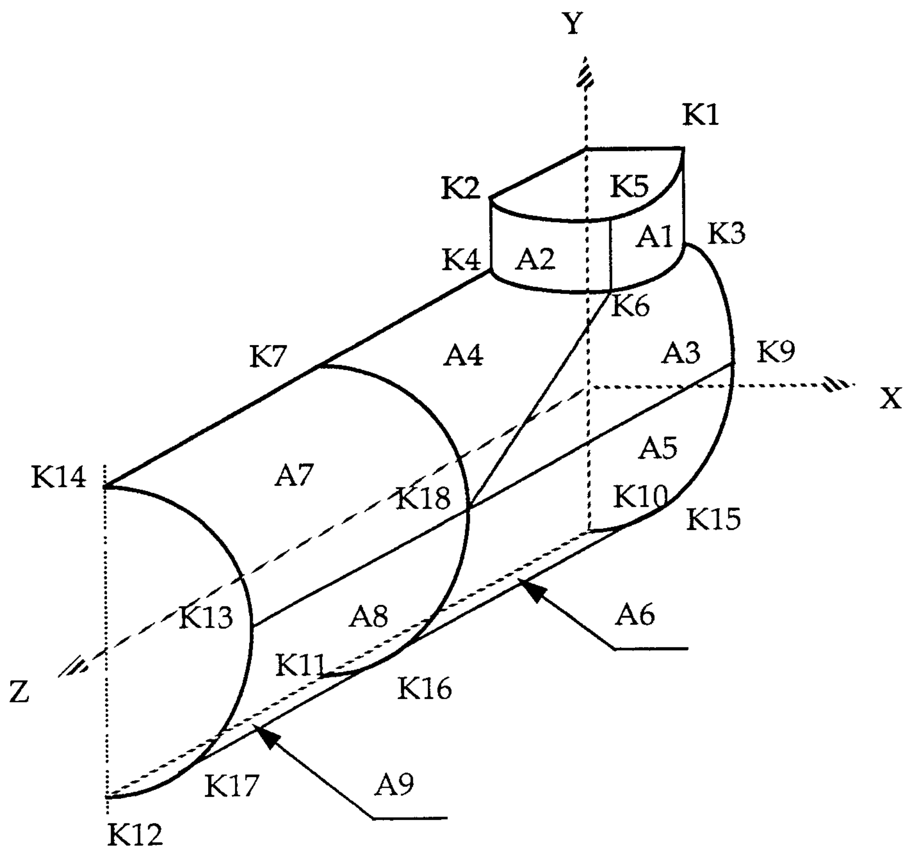

Figure 5. Areas and Keypoints at edge of model

Table 5. Results of the plots

No.	Point	Location/ Direction	Plot name	Stress factor
1	A	pipe/circumferential	pipe1-1	bending moment $M_{\phi p}/P$ on the pipe
2	A	pipe/longitudinal	pipe1-2	bending moment M_{xp}/P on the pipe
3	A	pipe/longitudinal	pipe1-3	Membrane force $N_{xp}/(P/R_p)$ on the pipe
4	A	pipe/circumferential	pipe1-4	Membrane force $N_{\phi p}/(P/R_p)$ on the pipe
5	C	pipe/longitudinal	pipe2-1	Bending moment M_{xp}/P on the pipe
6	C	pipe/circumferential	pipe2-2	Bending moment $M_{\phi p}/P$ on the pipe
7	C	pipe/circumferential	pipe2-3	Membrane force $N_{\phi p}/(P/R_p)$ on the pipe
8	C	pipe/longitudinal	pipe2-4	Membrane force $N_{xp}/(P/R_p)$ on the pipe
9	E	nozzle/circumferential	nozzle1-1	Bending moment $M_{\phi n}/P$ on the nozzle
10	E	nozzle/longitudinal	nozzle1-2	Bending moment M_{xn}/P on the nozzle
11	E	nozzle/longitudinal	nozzle1-3	Membrane force $N_{xn}/(P/r_n)$ on the nozzle
12	E	nozzle/circumferential	nozzle1-4	Membrane force $N_{\phi n}/(P/r_n)$ on the nozzle
13	G	nozzle/longitudinal	nozzle2-1	Bending moment M_{xn}/P on the nozzle

Table 5. Results of the plots

No.	Point	Location/ Direction	Plot name	Stress factor
14	G	nozzle/circumferential	nozzle2-2	Bending moment $M_{\phi n}/P$ on the nozzle
15	G	nozzle/circumferential	nozzle2-3	Membrane force $N_{\phi n}/(P/r_n)$ on the nozzle
16	G	nozzle/longitudinal	nozzle2-4	Membrane force $N_{xn}/(P/r_n)$ on the nozzle

CHAPTER V
COMPARISON AND CONCLUSION

In recent publications by Sun and Sun [8] [9], in order to focus their attention on the local stresses of the pipe, have assumed that the nozzle and pipe have the same wall thickness. However, for many nozzle-pipe connections, the nozzles have a smaller wall thickness than the pipes. There is no certainy the maximum stress will always occur on the pipe portion.

5.1 COMPARISON OF STRESS

The bending stress and membrane stress are considered separately.

5.1.1. Bending Stress

To investigate the location of the maximum bending stress, three gamma cases (10,50,and 100) and four beta cases (0.1, 0.3, 0.6, and 0.9) are used for comparison as shown in Table 6.

From Table 6, it is noted that the maximum bending stress location will shift from pipe to nozzle when β and Υ values increase.

Table 6. Comparison of Bending Stresses (psi) when $t=\beta T$

Υ	Point	Location	$\beta = 0.1$	$\beta = 0.3$	$\beta = 0.6$	$\beta = 0.9$
$\Upsilon=10$	A	pipe	-35073.4	-11577.1	-5168.39	-2978.26
	C	pipe	-27463.5	-6757.0	-912.1	406.632
	E	nozzle	-13429.0	-9505.6	-1883.4	-556.69
	G	nozzle	-13956.0	-7251.6	-1013.3	817.1001
Max. stress location			A pipe	A pipe	A pipe	A pipe

Table 6. Comparison of Bending Stresses (psi) when t=βT

ϒ	Point	Location	β = 0.1	β =0.3	β =0.6	β = 0.9
ϒ=50	A C E G	pipe pipe nozzle nozzle	-18360.8 -11499.2 -8612.0 -6088.5	-3814.7 -2520.5 -7175.3 -3441.0	-867.49 -733.5 -2059.34 -673.7	-269.41 -287.65 -730.86 -26.71
Max. stress location			A pipe	E nozzle	E nozzle	E nozzle
ϒ=100	A C E G	pipe pipe nozzle nozzle	-13034.7 -7044.6 -6409.0 -3844.2	-2247.9 -1661.2 -5287.6 -2169.2	-225.3 -512.61 -1152.55 -386.56	-36.91 -235.621 -326.69 -17.94
Max. stress location			A pipe	E nozzle	E nozzle	E nozzle

5.1.2. Membrane Stress

To investigate the membrane stress at the nozzle-pipe connection, the same combinations of gamma and beta are used as shown in Table 7.

Table 7. Comparison of Membrane Stresses (psi) when t=βT

ϒ	Point	Location	β = 0.1	β = 0.3	β = 0.6	β = 0.9
ϒ =10	A C E G	pipe pipe nozzle nozzle	-8431.6 -6889.5 -22621.0 -20594.0	-46.0 -5397.0 -7221.4 -7902.4	-900.71 -2691.9 -1637.0 -3214.5	-135.04 -453.12 -397.86 -814.41
Max. stress location			E nozzle	G nozzle	G nozzle	G nozzle
ϒ=50	A C E G	pipe pipe nozzle nozzle	-7487.2 -6885.8 -13002.0 -9982.5	-2390.8 -3945.9 -4504.7 -5064.4	-537.51 -1234.7 -699.26 -1479.8	-321.86 -319.74 -126.72 -324.88
Max. stress location			E nozzle	G nozzle	G nozzle	G nozzle
ϒ=100	A C E G	pipe pipe nozzle nozzle	-5977.3 -6570.4 -9044.0 -6816.8	-1625.5 -3165.6 -3512.3 -2787.0	-613.86 -792.69 -860.85 -985.91	-395.03 -46.999 -589.13 -178.91
Max. stress location			E nozzle	E nozzle	G nozzle	E nozzle

It is noted that the maximum membrane stress occur on the nozzle when the nozzle wall thickness is less than the pipe wall thickness.

5.2 COMPARISON OF STRESS FACTOR

5.2.1.Stress factor on the pipe

1, In general, all stress factors are decreasing when β and Υ are increasing.

2, When the β value is large, the value of gamma is less significant to the value of stress factors.

5.2.2. Stress Factor on the Nozzle

1, The membrane stresses are more significant than the bending stresses, since radial loads are applied downward from the nozzle to the pipe. In addition, the values of stress factors increase as β and Υ increase. It can be seen from Figures 16, 17, 20 and 21.

2, Stress factors at point G, when the symmetric transverse plan intersects the pipe, may decrease when β is larger than 0.6.

5.3 CONCLUSION

Maximum stress does not always occur on the pipe. When the wall thickness of the nozzle is less than the wall thickness of pipe, the maximum stress location shifts from the pipe to the nozzle.

APPENDIX A. PLOTS OF STRESS FACTOR

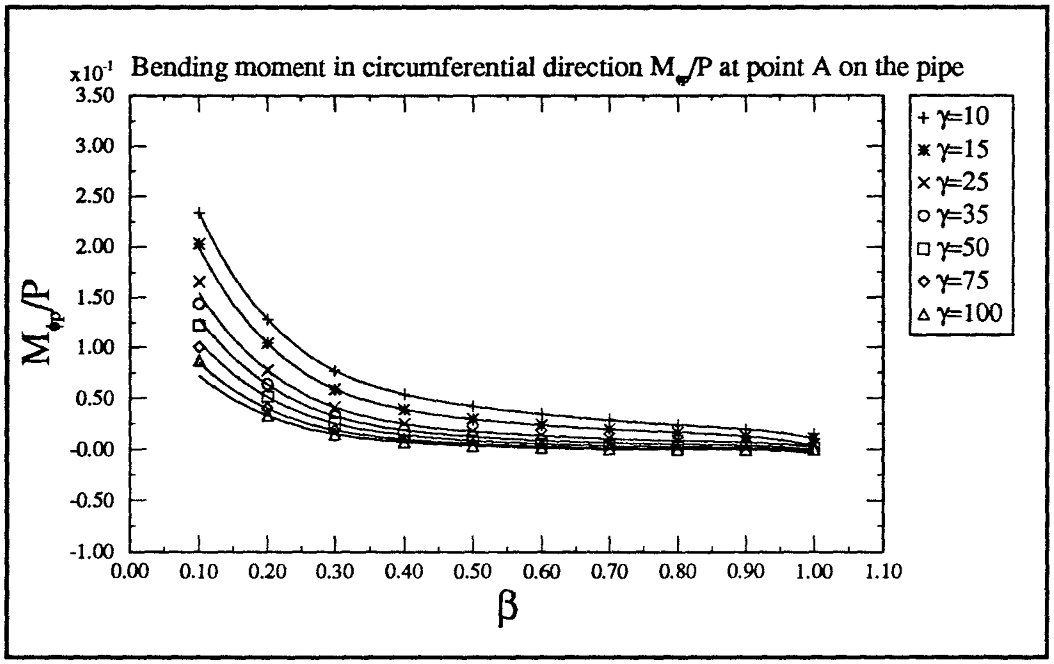

Figure 6 Pipe1-1

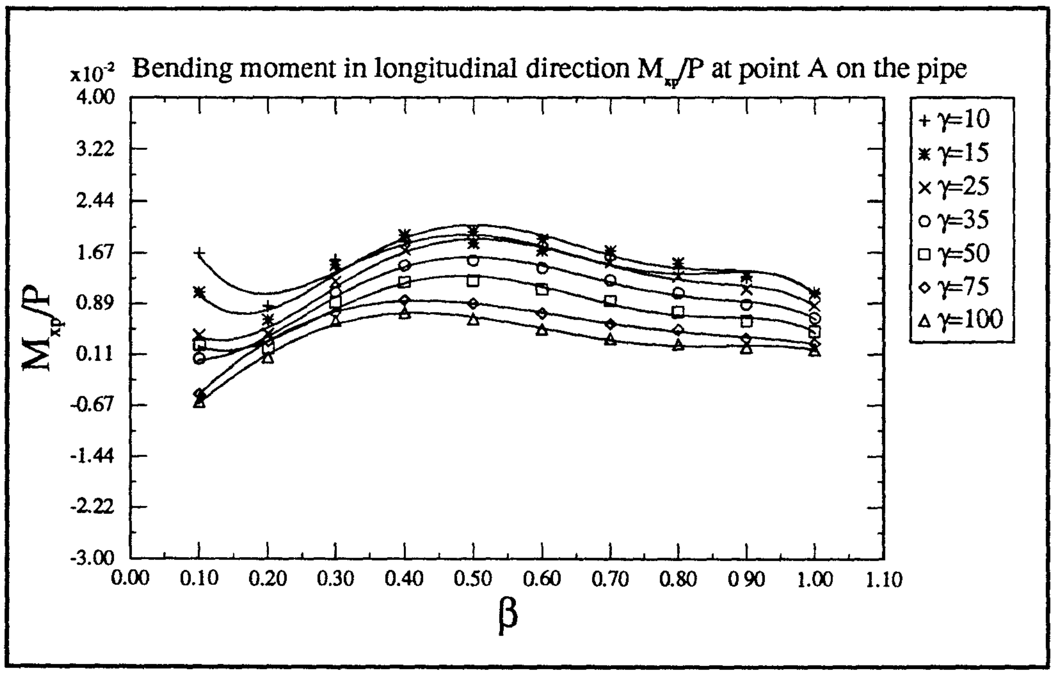

Figure 7 Pipe1-2

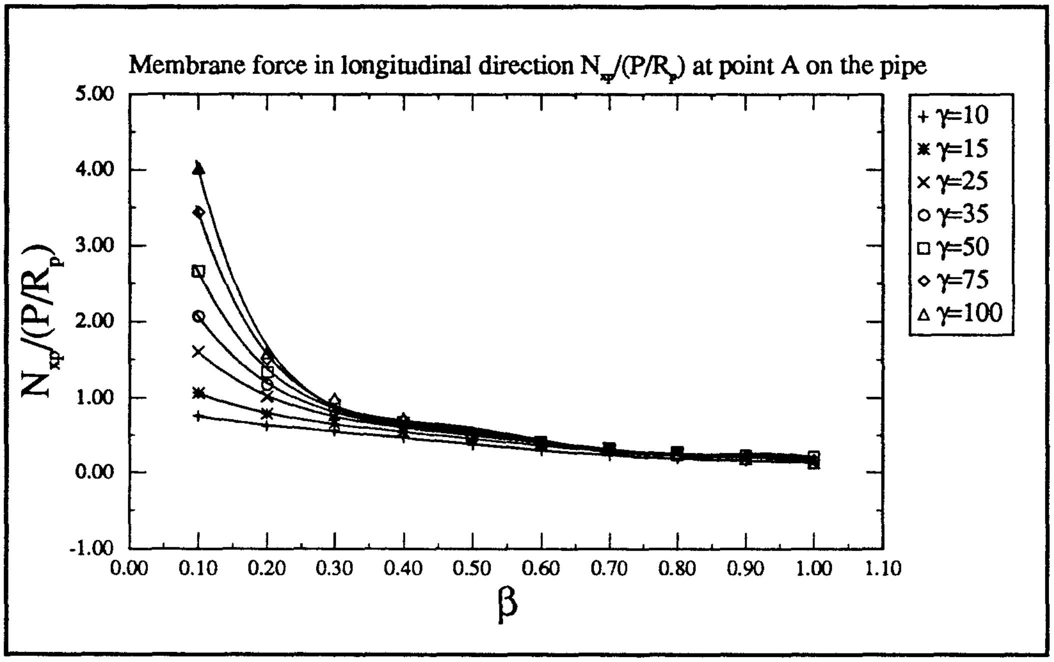

Figure 8 Pipe1-3

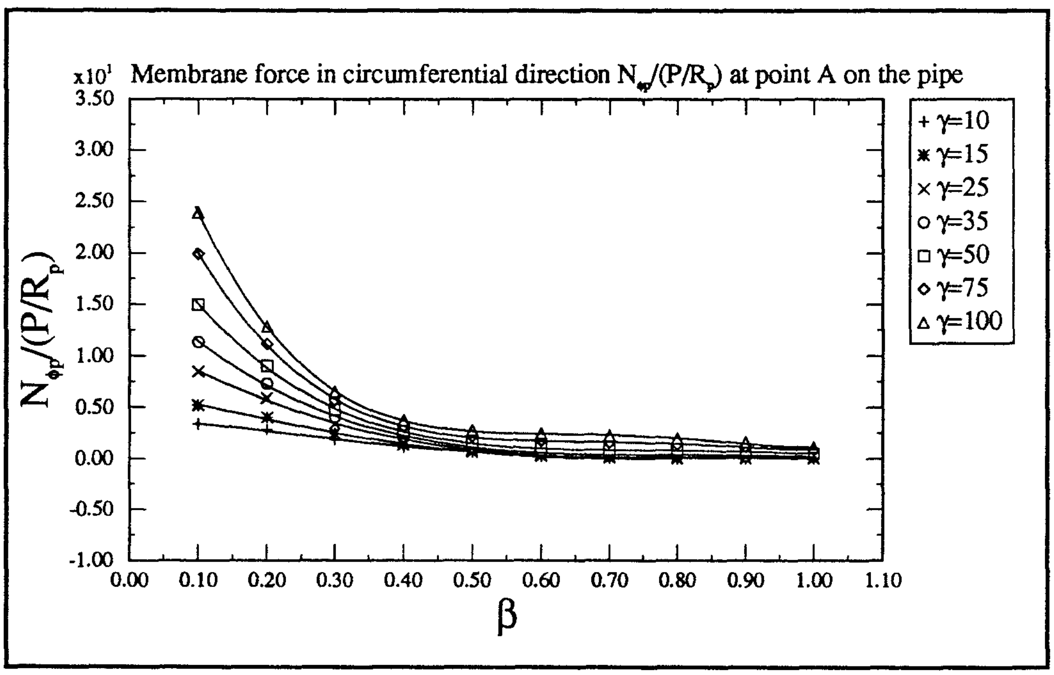

Figure 9 Pipe1-4

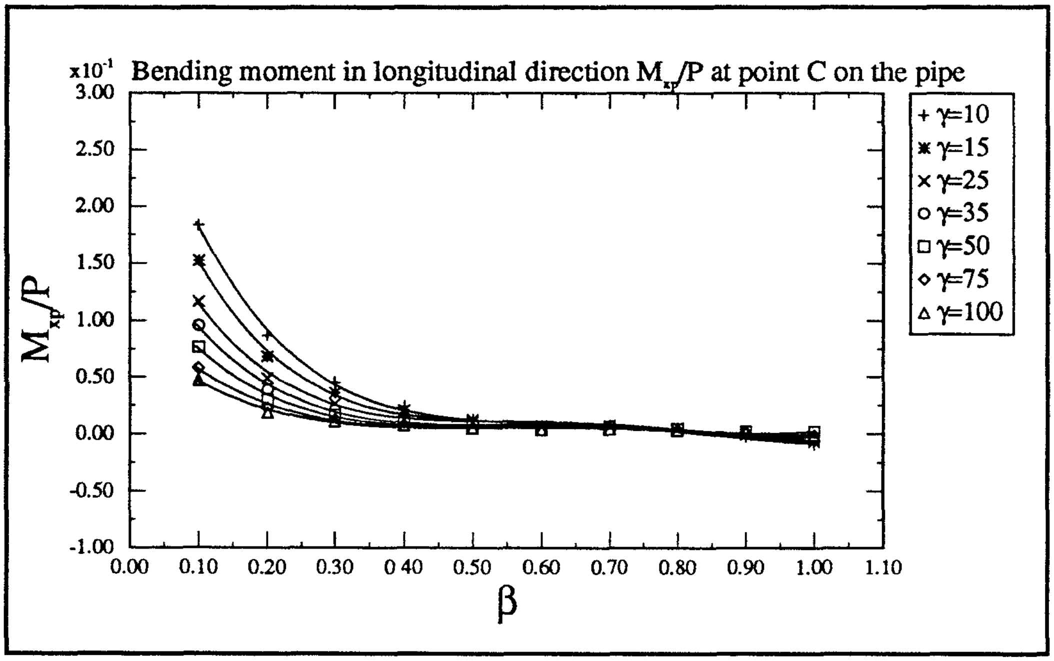

Figure 10 Pipe2-1

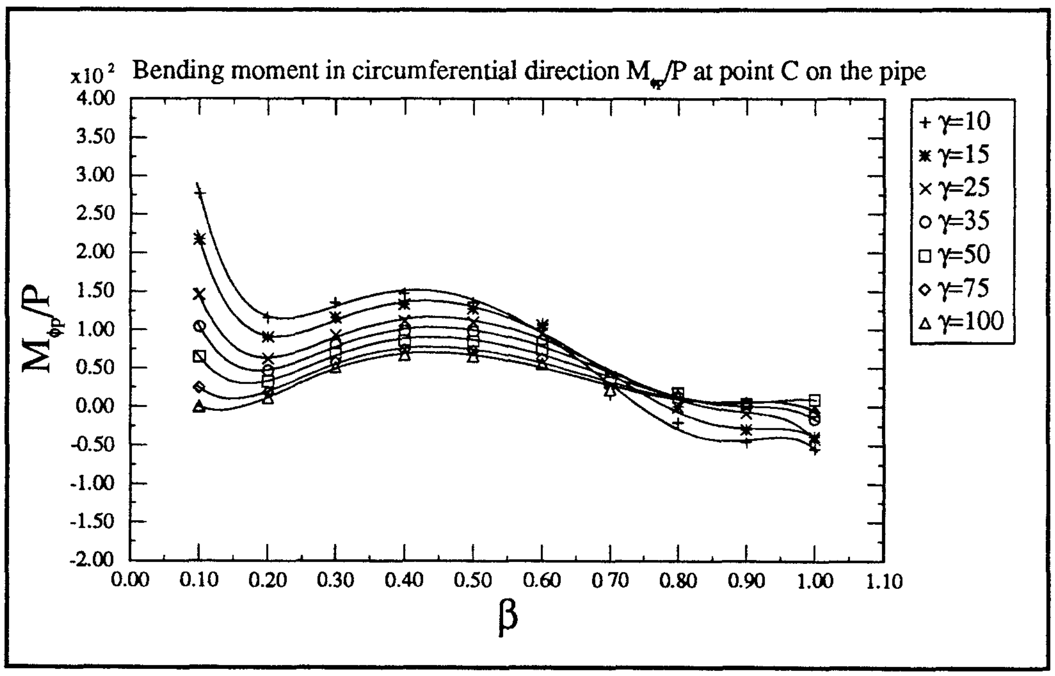

Figure 11 Pipe2-2

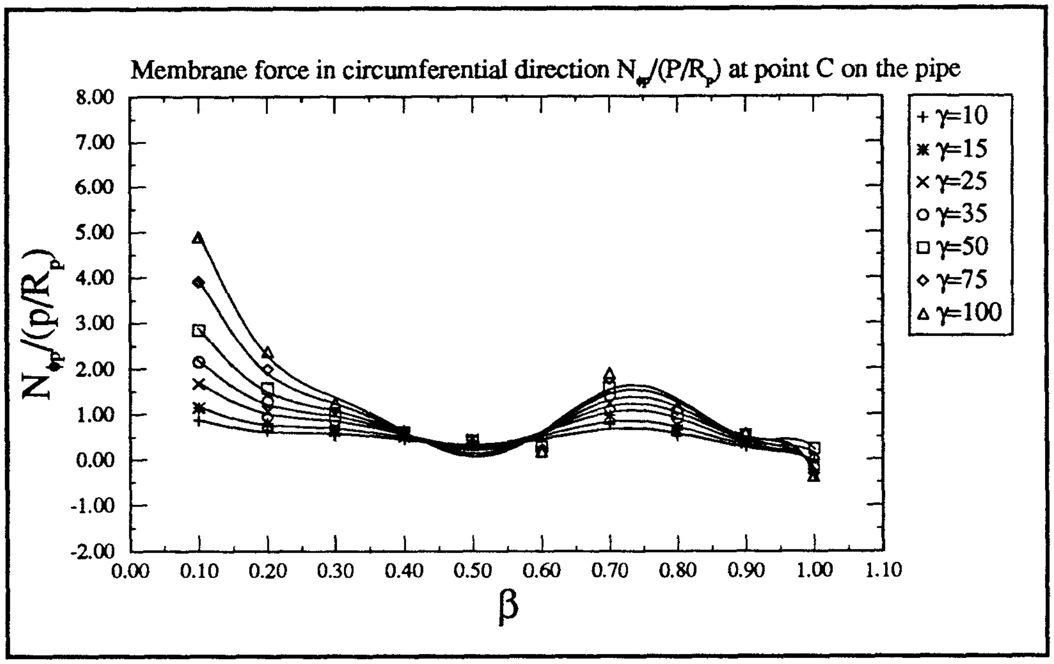

Figure 12 Pipe2-3

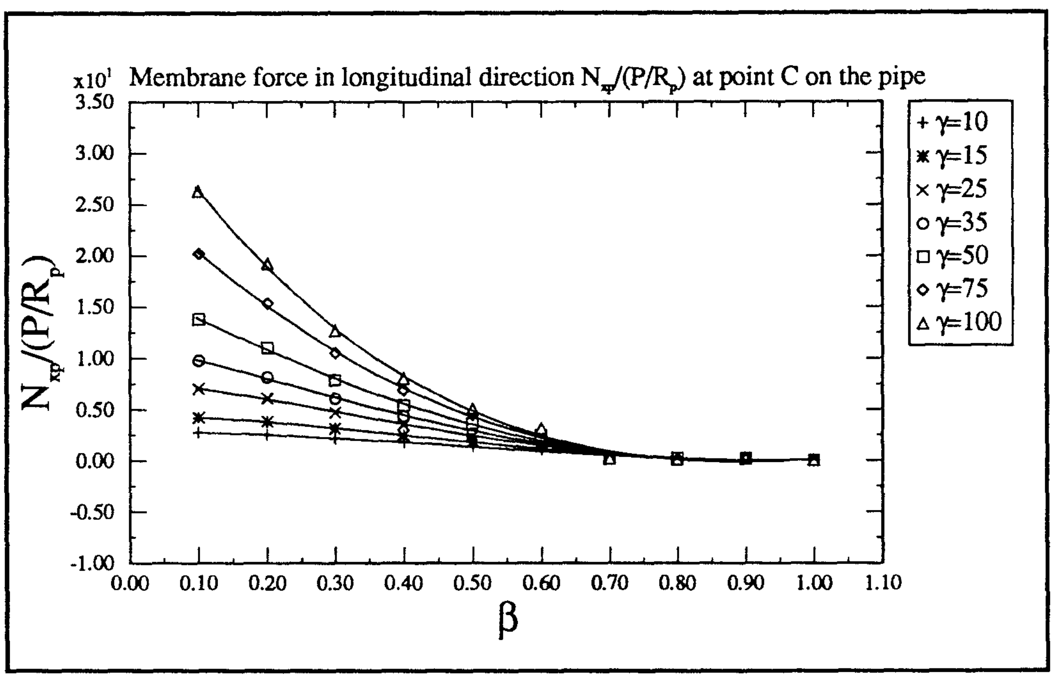

Figure 13 Pipe2-4

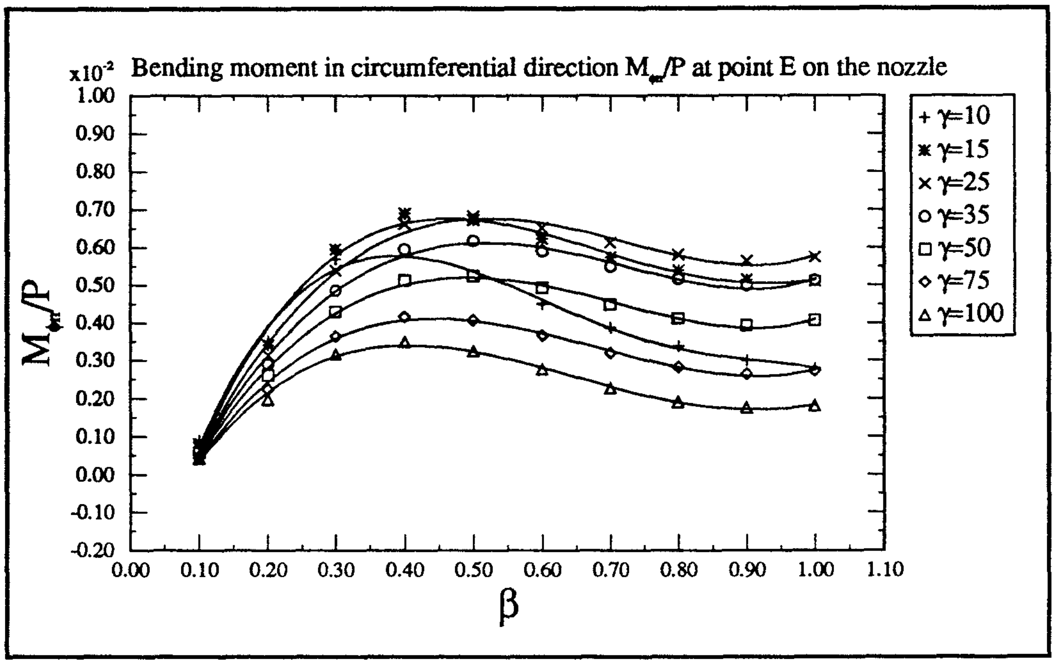

Figure 14 Nozzle1-1

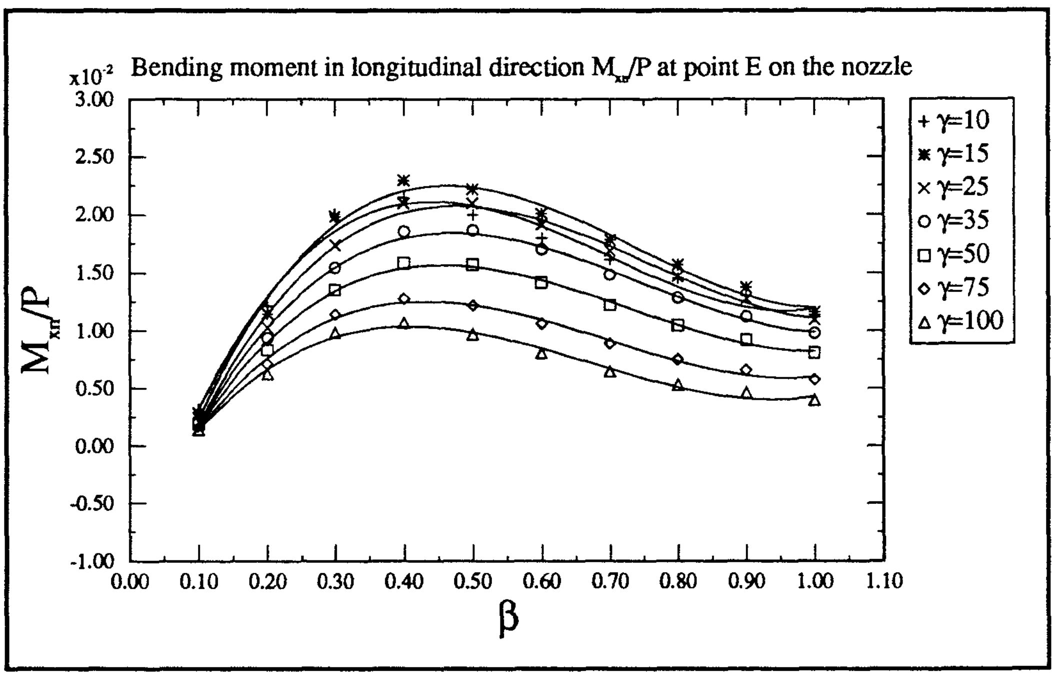

Figure 15 Nozzle1-2

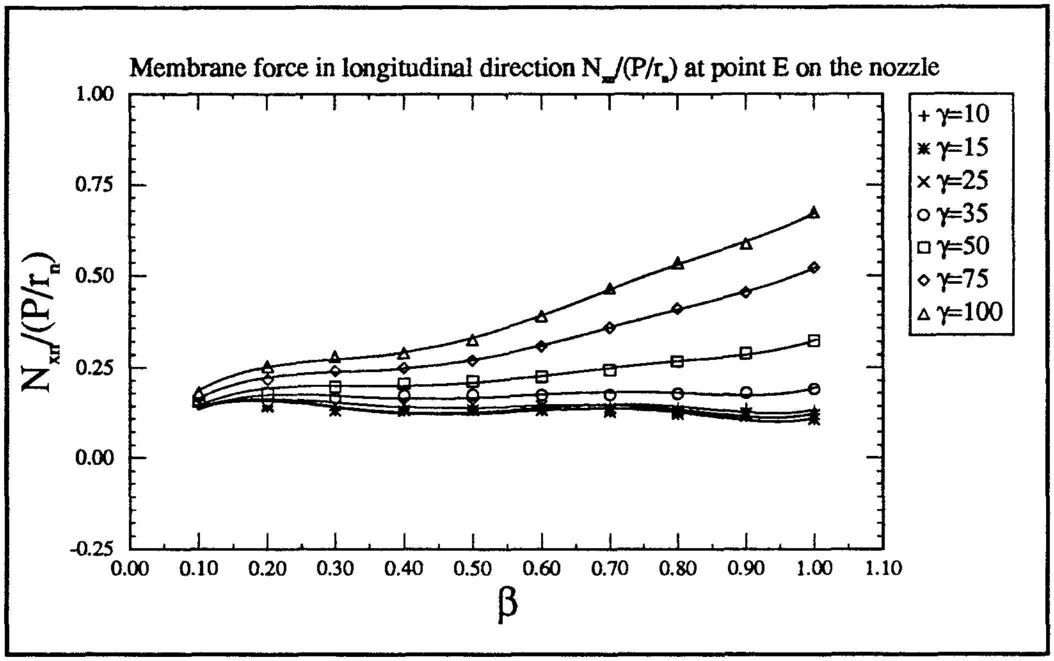

Figure 16 Nozzle1-3

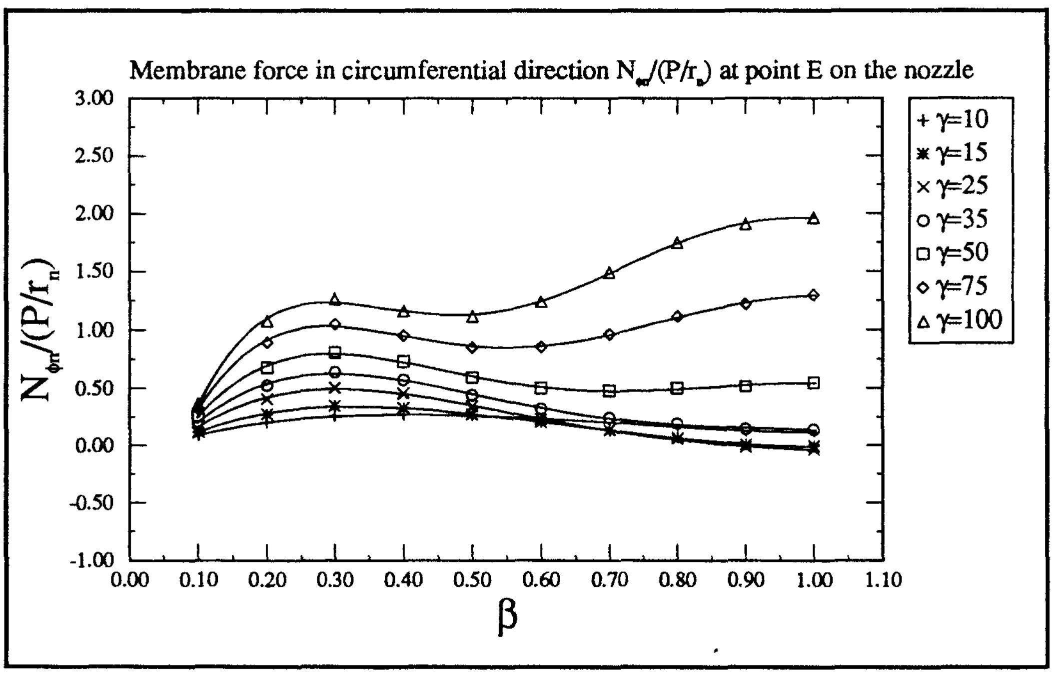

Figure 17 Nozzle1-4

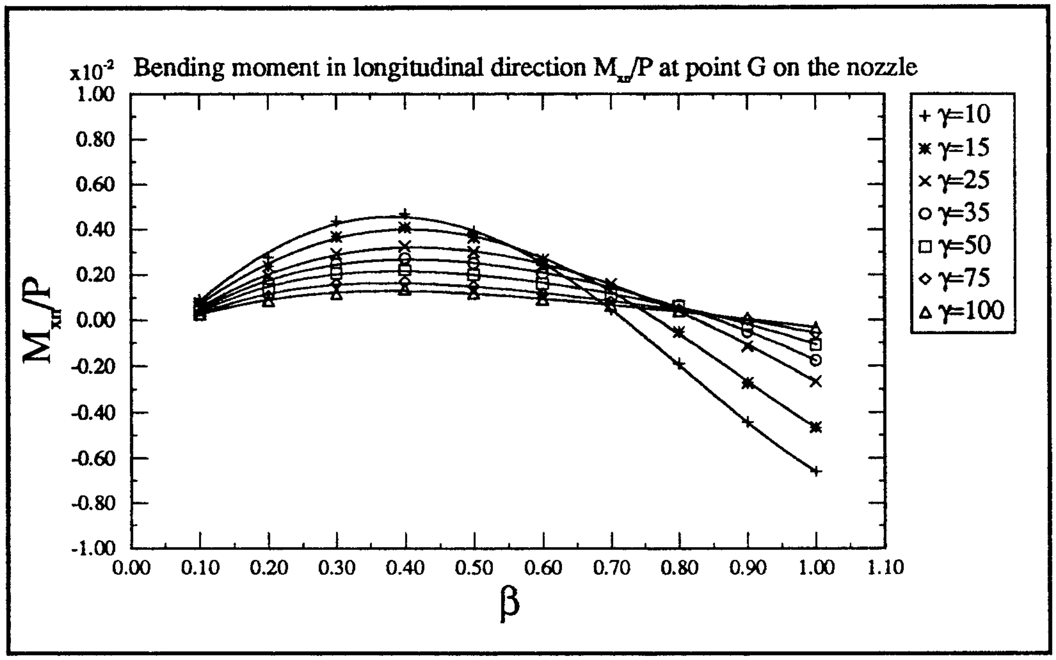

Figure 18 Nozzle2-1

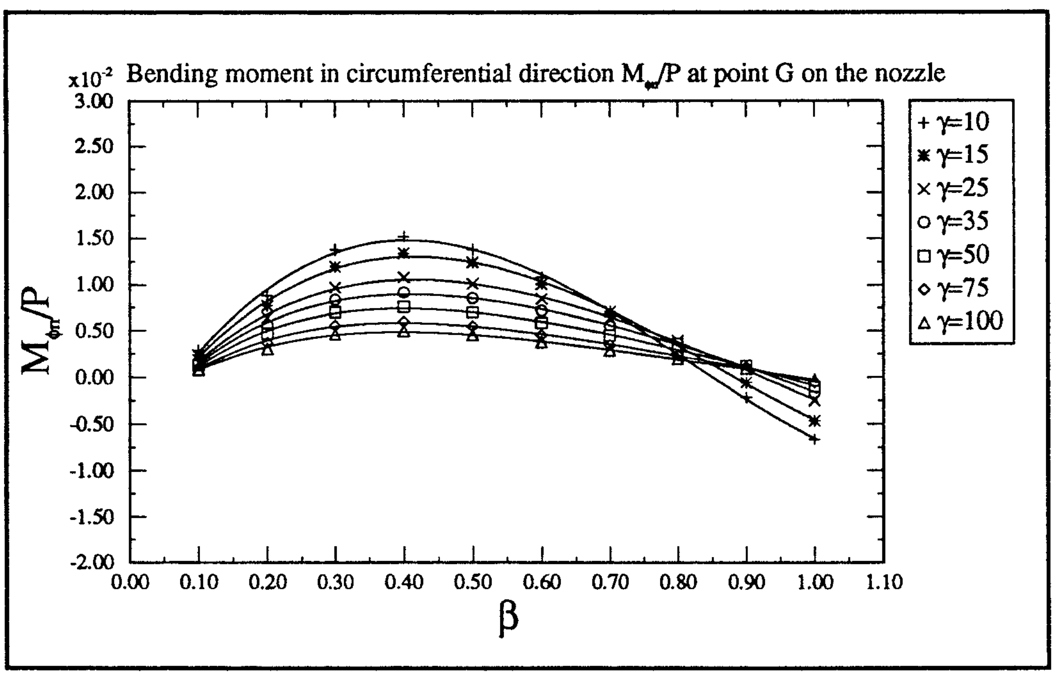

Figure 19 Nozzle2-2

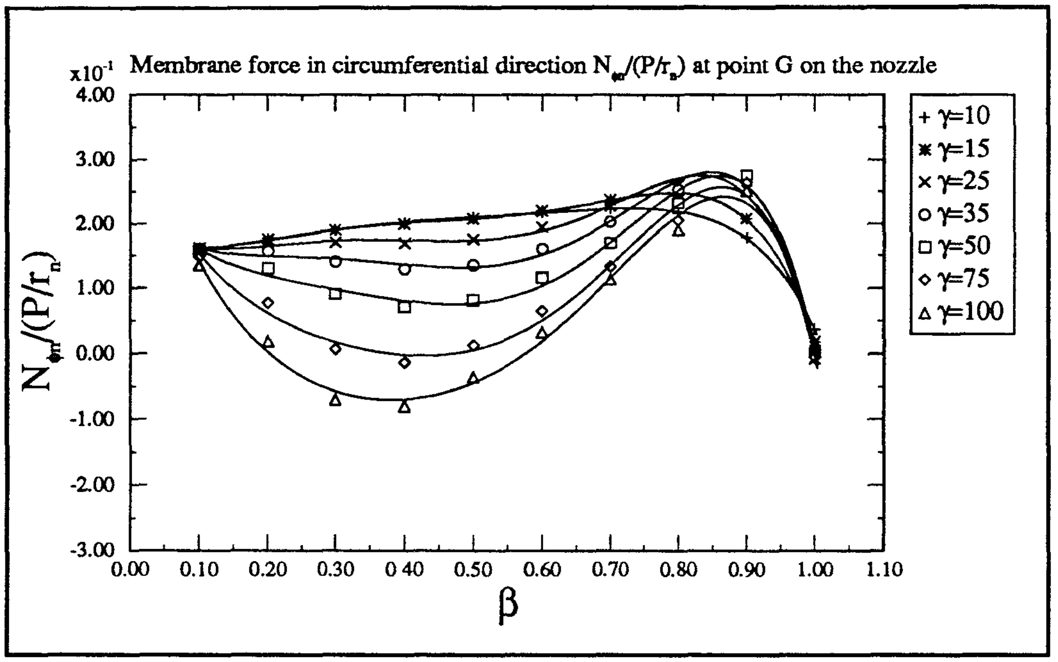

Figure 20 Nozzle2-3

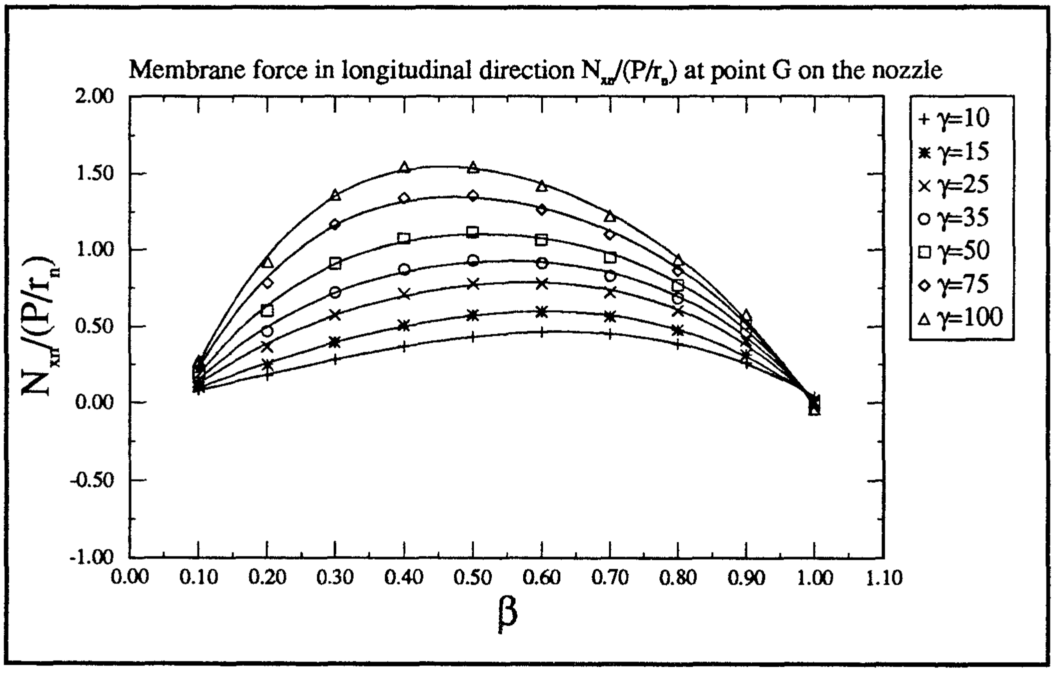

Figure 21 Nozzle2-4

APPENDIX B. DATA

β = 0.1, 0.2, 0.3, 0.4, 0.5, 0.6, 0.7, 0.8, 0.9, 1.0

Υ = 10, 15, 25, 35, 50, 75, 100

Pipe1-1

0.10 0.233823 0.203305 0.166067 0.143839 0.122405 0.100585
0.086898
0.20 0.128238 0.104269 0.077667 0.063540 0.051264 0.039845
0.033050
0.30 0.077181 0.058908 0.041004 0.032485 0.025431 0.018914
0.014986
0.40 0.053957 0.038945 0.025002 0.019021 0.014385 0.010103
0.007436
0.50 0.042071 0.029577 0.017657 0.012629 0.008898 0.005606
0.003611
0.60 0.034456 0.023983 0.013555 0.009062 0.005783 0.003049
0.001502
0.70 0.028720 0.019913 0.010774 0.006737 0.003832 0.001560
0.000389
0.80 0.024003 0.016627 0.008694 0.005115 0.002584 0.000748
-0.000100
0.90 0.019855 0.012992 0.007040 0.003952 0.001796 0.000343
-0.000246
1.00 0.015399 0.010650 0.005226 0.002657 0.000901 0.000145
-0.000476

Pipe1-2

0.10 0.016651 0.010625 0.004037 0.000472 0.002556 -0.005027

-0.006182

0.20 0.008471 0.006391 0.004205 0.003042 0.002028 0.003123

0.000601

0.30 0.015561 0.014763 0.012236 0.010602 0.009093 0.007398

0.006128

0.40 0.018411 0.019340 0.017036 0.014671 0.012173 0.009412

0.007451

0.50 0.018131 0.019867 0.018063 0.015472 0.012403 0.008882

0.006487

0.60 0.016919 0.018639 0.016956 0.014313 0.011068 0.007334

0.004885

0.70 0.015572 0.016884 0.015065 0.012426 0.009240 0.005704

0.003499

0.80 0.014240 0.015023 0.013042 0.010501 0.007546 0.004848

0.002634

0.90 0.012796 0.013069 0.011059 0.008753 0.006166 0.003605

0.002202

1.00 0.010603 0.010451 0.008570 0.006653 0.004621 0.002750

0.001797

Pipe1-3

0.10 0.756640 1.063980 1.605200 2.070180 2.660600 3.432600

4.013200

0.20 0.629520 0.789660 1.016900 1.175510 1.341640 1.506990

1.589240

0.30 0.566760 0.662940 0.767910 0.837144 0.906440 0.968010

0.993600

0.40 0.473400 0.555162 0.613700 0.643384 0.676300 0.710520

0.723800

0.50 0.377072 0.450492 0.493560 0.507682 0.523340 0.540300

0.540480

0.60 0.298200 0.362082 0.397030 0.405174 0.412900 0.417660
0.405360
0.70 0.238124 0.292722 0.321940 0.327698 0.331620 0.328140
0.307468
0.80 0.193208 0.239700 0.265040 0.270200 0.272240 0.263364
0.238836
0.90 0.158772 0.198342 0.221890 0.227808 0.228820 0.215760
0.189972
1.00 0.134276 0.174408 0.209060 0.219394 0.213000 0.175512
0.129592

Pipe1-4

0.10 3.372640 5.214120 8.487000 11.328940 14.974400
19.908600 23.909200
0.20 2.857720 4.038420 5.885000 7.329000 9.032800
11.161500 12.817200
0.30 1.853560 2.468880 3.408800 4.067560 4.781600
5.702100 6.502000
0.40 1.093760 1.316280 1.778900 2.154180 2.571000
3.145500 3.729960
0.50 0.631920 0.647580 0.863910 1.140020 1.527340
2.141970 2.771640
0.60 0.360284 0.289224 0.406000 0.658364 1.075020
1.773960 2.455440
0.70 0.199572 0.100866 0.189750 0.444066 0.881580
1.595490 2.243400
0.80 0.105600 0.005578 0.089370 0.340606 0.766120
1.415850 1.955200
0.90 0.054016 0.034823 0.043735 0.272804 0.649760
1.182000 1.580120
1.00 0.043588 0.015037 0.057759 0.235914 0.512480

0.870240 1.108320

Pipe2-1

0.10 0.183090 0.152124 0.116515 0.095896 0.076661
0.058068 0.046964
0.20 0.087423 0.068345 0.048935 0.039020 0.030483
0.022810 0.018536
0.30 0.045047 0.035915 0.026157 0.021065 0.016803
0.013082 0.011088
0.40 0.023831 0.020514 0.020514 0.013161 0.010697
0.008597 0.007488
0.50 0.012557 0.012155 0.010331 0.008732 0.007201
0.005846 0.005117
0.60 0.006081 0.007069 0.006710 0.005860 0.004890
0.003948 0.003417
0.70 0.007004 0.007595 0.007443 0.006805 0.005938
0.005002 0.004424
0.80 0.002597 0.004007 0.004872 0.004731 0.004209
0.003500 0.003036
0.90 -0.002711 -0.000699 0.001193 0.001778 0.001918
0.001754 0.001571
1.00 -0.008617 -0.006420 -0.003968 -0.002821 0.001993
-0.001404 -0.001112

Pipe2-2

0.10 0.027654 0.021709 0.014580 0.010411 0.006453
0.002475 0.000003
0.20 0.011582 0.009045 0.006233 0.004653 0.003221
0.001872 0.001100
0.30 0.013548 0.011602 0.009286 0.008043 0.006892

0.005766 0.005129

0.40 0.014754 0.013348 0.011162 0.009841 0.008604

0.007413 0.006728

0.50 0.013582 0.012733 0.011011 0.009761 0.008507

0.007283 0.006565

0.60 0.010809 0.010623 0.009586 0.008562 0.007422

0.006271 0.005579

0.70 0.001547 0.003219 0.003905 0.003665 0.003167

0.002582 0.002230

0.80 -0.002019 -0.000019 0.001503 0.001829 0.001781

0.001521 0.001317

0.90 -0.004591 -0.002908 -0.000835 -0.000057 0.000382

0.000547 0.000546

1.00 -0.005368 -0.003810 -0.004131 -0.001526 0.000985

-0.000611 -0.000422

Pipe2-3

0.10 0.866760 1.144800 1.666300 2.153060 2.842400

3.906900 4.892400

0.20 0.650320 0.811980 1.073700 1.288546 1.573440

1.995240 2.381960

0.30 0.543000 0.638820 0.775660 0.869120 0.975000

1.118190 1.249560

0.40 0.457120 0.514134 0.574840 0.600068 0.614920

0.626850 0.641360

0.50 0.388684 0.424740 0.443330 0.432264 0.403540

0.359940 0.327732

0.60 0.338676 0.366990 0.366630 0.338814 0.292440

0.231141 0.186736

0.70 0.779480 0.973860 1.232300 1.404200 1.583260

1.773630 1.891520

0.80 0.530800 0.650400 0.812500 0.914886 1.010980
1.098810 1.146480
0.90 0.284208 0.354756 0.423860 0.483350 0.533560
0.561750 0.562480
1.00 -0.030114 -0.077868 0.141600 -0.183764 0.231080
-0.306450 -0.365748

Pipe2-4

0.10 2.755800 4.224240 7.041700 9.765840 13.771600
20.198400 26.281600
0.20 2.567840 3.845520 6.121700 8.171800 11.033000
15.366900 19.224400
0.30 2.158800 3.135480 4.734900 6.085240 7.891800
10.491300 12.662400
0.40 1.753440 2.447940 3.508500 4.354280 5.438600
6.911100 8.054400
0.50 1.396280 1.869540 2.550100 3.063060 3.688400
4.486800 5.065600
0.60 1.076760 1.388280 1.816300 2.121000 2.469400
2.885160 3.170760
0.70 0.304300 0.335712 0.338080 0.310772 0.265920
0.210090 0.172992
0.80 0.249920 0.283080 0.296060 0.275520 0.233400
0.174054 0.130916
0.90 0.181248 0.212820 0.252410 0.263074 0.253440
0.219972 0.187996
1.00 0.049128 0.038405 0.036926 0.041793 0.050430
0.048354 0.051720

Nozzle1-1

0.10 0.000895 0.000823 0.000723 0.000653 0.000574 0.000486
0.000427
0.20 0.003515 0.003419 0.003140 0.002901 0.002607 0.002244
0.001983
0.30 0.005703 0.005956 0.005397 0.004867 0.004305 0.003652
0.003173
0.40 0.005910 0.006901 0.006627 0.005957 0.005135 0.004175
0.003499
0.50 0.005265 0.006727 0.006822 0.006181 0.005254 0.004086
0.003254
0.60 0.004520 0.006229 0.006522 0.005909 0.004942 0.003679
0.002766
0.70 0.003885 0.005752 0.006127 0.005503 0.004501 0.003201
0.002268
0.80 0.003388 0.005395 0.005818 0.005170 0.004135 0.002830
0.001914
0.90 0.003006 0.005156 0.005652 0.005001 0.003947 0.002647
0.001764
1.00 0.002793 0.005105 0.005750 0.005138 0.004071 0.002720
0.001814

Nozzle1-2

0.10 0.003188 0.002870 0.002478 0.002216 0.001932
0.001617 0.001411
0.20 0.012142 0.011438 0.010250 0.009368 0.008346
0.007122 0.006254
0.30 0.020031 0.019848 0.017390 0.015480 0.013555
0.011403 0.009858
0.40 0.021495 0.022956 0.020987 0.018571 0.015849
0.012791 0.010682
0.50 0.019995 0.022190 0.020989 0.018670 0.015731

0.012195 0.009714
0.60 0.017981 0.020104 0.019184 0.017034 0.014180
0.010621 0.008062
0.70 0.016145 0.017842 0.016890 0.014882 0.012225
0.008898 0.006470
0.80 0.014548 0.015732 0.014705 0.012877 0.010492
0.007518 0.005328
0.90 0.013033 0.013757 0.012783 0.011234 0.009184
0.006583 0.004653
1.00 0.011190 0.011611 0.010956 0.009807 0.008107
0.005752 0.003990

Nozzle1-3

0.10 0.156748 0.155406 0.154450 0.155022 0.158160
0.167673 0.180232
0.20 0.144627 0.142363 0.147264 0.158379 0.179592
0.217188 0.253280
0.30 0.133934 0.131674 0.146304 0.166912 0.197118
0.241782 0.280818
0.40 0.133504 0.130877 0.148923 0.173524 0.205971
0.249984 0.290470
0.50 0.136510 0.132586 0.148650 0.175070 0.213395
0.270503 0.326390
0.60 0.138627 0.131756 0.144252 0.174334 0.225259
0.309150 0.390946
0.70 0.139099 0.127969 0.137778 0.175115 0.244216
0.359694 0.466813
0.80 0.138051 0.121974 0.130707 0.178071 0.267558
0.411418 0.535859
0.90 0.135503 0.114390 0.122990 0.180590 0.288959
0.454799 0.588416

1.00 0.131176 0.107388 0.120340 0.191226 0.323620
0.522570 0.674800

Nozzle1-4

0.10 0.090484 0.117234 0.165830 0.207900 0.260040 0.322050
0.361760
0.20 0.198752 0.275424 0.409320 0.526540 0.681160 0.897120
1.075184
0.30 0.259970 0.348160 0.507051 0.641050 0.810846 1.052082
1.264428
0.40 0.272794 0.329942 0.456960 0.576710 0.732192 0.955728
1.162496
0.50 0.260850 0.272505 0.344700 0.442960 0.595350 0.852000
1.114800
0.60 0.235728 0.204444 0.231307 0.323634 0.503467 0.855382
1.239624
0.70 0.202742 0.135237 0.135769 0.244079 0.482180 0.966069
1.490776
0.80 0.165862 0.068575 0.056057 0.192954 0.502374 1.113792
1.747200
0.90 0.128907 0.007920 -0.015082 0.146898 0.517979 1.221804
1.908781
1.00 0.120296 -0.006147 -0.037151 0.138114 0.549680 1.297380
1.963560

Nozzle2-1

0.10 0.000930 0.000761 0.000592 0.000497 0.000406
0.000314 0.000256
0.20 0.002780 0.002374 0.001941 0.001666 0.001383
0.001076 0.000874

0.30	0.004351	0.003680	0.002926	0.002496	0.002065	0.001600	0.001182
0.40	0.004682	0.004092	0.003261	0.002736	0.002223	0.001700	0.001378
0.50	0.003910	0.003654	0.003025	0.002525	0.002012	0.001503	0.001204
0.60	0.002432	0.002683	0.002435	0.002054	0.001617	0.001179	0.000928
0.70	0.000456	0.001300	0.001596	0.001437	0.001150	0.000830	0.000645
0.80	-0.001888	-0.000503	0.000476	0.000666	0.000630	0.000489	0.000391
0.90	-0.004412	-0.002716	-0.001131	-0.000505	-0.000144	0.000038	0.000097
1.00	-0.006588	-0.004651	-0.002665	-0.001752	-0.001078	-0.000570	-0.000324

Nozzle2-2

0.10	0.002861	0.002360	0.001852	0.001562	0.001284	0.001003	0.000827
0.20	0.008813	0.007705	0.006429	0.005572	0.004671	0.003693	0.003046
0.30	0.013819	0.011977	0.009717	0.008386	0.007030	0.005558	0.004610
0.40	0.015214	0.013431	0.010813	0.009198	0.007620	0.005999	0.004992
0.50	0.013797	0.012427	0.010129	0.008567	0.007019	0.005479	0.004557
0.60	0.010834	0.010105	0.008485	0.007194	0.005854	0.004531	0.003758
0.70	0.006995	0.007079	0.006371	0.005500	0.004485		

0.003456 0.002863
0.80 0.002627 0.003558 0.003924 0.003613 0.003033
0.002356 0.001952
0.90 -0.002155 -0.000560 0.000837 0.001211 0.001251
0.001094 0.000958
1.00 -0.006619 -0.004629 -0.002457 -0.001619 -0.000963
-0.000498 -0.000280

Nozzle2-3

0.10 0.160620 0.161268 0.161140 0.160062 0.156912
0.147804 0.134824
0.20 0.173360 0.175080 0.169184 0.156481 0.130336
0.076904 0.018776
0.30 0.189958 0.190382 0.170253 0.140591 0.090671
0.006847 -0.069736
0.40 0.202029 0.200198 0.169216 0.129716 0.071312
-0.012664 -0.079405
0.50 0.210570 0.208125 0.175283 0.135485 0.081475
0.012941 -0.035571
0.60 0.217886 0.220255 0.194825 0.160650 0.116179
0.065344 0.033018
0.70 0.223362 0.236867 0.227664 0.203227 0.169560
0.133335 0.113190
0.80 0.217444 0.244604 0.261030 0.252968 0.232486
0.205747 0.190500
0.90 0.177863 0.208504 0.252088 0.270924 0.275400
0.263898 0.251453
1.00 0.037288 0.018344 -0.007007 0.005975 0.003682
-0.004822 0.010216

Nozzle2-4

0.10	0.082376	0.101022	0.134290	0.163198	0.199650	0.243501	0.272672
0.20	0.180672	0.248856	0.366900	0.469078	0.602920	0.783384	0.921808
0.30	0.284486	0.396247	0.575271	0.722119	0.911592	1.167264	1.363320
0.40	0.372173	0.508493	0.714016	0.874070	1.074912	1.342272	1.546496
0.50	0.434690	0.576480	0.780300	0.931805	1.116100	1.357800	1.544100
0.60	0.462888	0.596095	0.780660	0.911786	1.065456	1.263708	1.419754
0.70	0.449526	0.565362	0.722946	0.830266	0.950022	1.100251	1.221472
0.80	0.386867	0.478349	0.605466	0.688370	0.772454	0.866266	0.937446
0.90	0.263869	0.318345	0.407398	0.467786	0.521413	0.562132	0.579668
1.00	0.039967	0.018479	-0.000335	-0.006838	-0.013984	-0.029918	-0.040792

APPENDIX C. ANSYS INPUT PROGRAM

```
/PREP7
KAN,0
/TITLE CASE-1 1/4 MODEL CIRCUMFERENTIAL DIRECTION
/COM RADIAL LOADING CIRCUMFERENTIAL DIRECTION
/COM BETA=0.30 GAMMA=10 T=0.2 t=T*BETA
/SHOW
*SET,PRSS,0
*SET,PLBS,-1000
*SET,BETA,0.30
*SET,GAMA,10
*SET,THNP,0.2
*SET,THNT,BETA*THNP
*SET,PLB1,PLBS*0.0052083
*SET,PLB2,PLB1*2
*SET,RPIP,THNP*GAMA
*SET,RTRU,BETA*RPIP
*SET,LENT,RPIP*0.1
*SET,LORT,RPIP*4
*SET,ANG,ACOS(BETA)
*SET,THED,(ANG-0.5236)*57.296
*SET,MIDD,(THED-90)/2
*SET,RPME,RPIP+LENT
*SET,MMEE,(2.10-ANG)
*SET,MECE,MMEE*RPIP
ET,1,63,,,,,,,1
EX,1,30E6
NUXY,1,0.3
ET,2,63,,,,,2
EX,2,30E6
NUXY,2,0.3
```

31. R,1,THNP
32. R,2,THNT
33. N,1 $,2,1 $,3,,,1
34. CS,11,1,1,3,2
35. NDELE,1,3,1
36. /VIEW,,1,1,1
37. CSYS,11
38. K,1,RTRU,90,RPME
39. K,2,RTRU,,RPME
40. K,3,RTRU,90,1
41. K,4,RTRU,,RPIP
42. KMOVE,3,11,RTRU,90,999,1,RPIP,999,0
43. KMOVE,4,11,RTRU,0,RPIP,1,RPIP,90,RTRU
44. L,1,3,4,0.3
45. L,2,4,4,0.3
46. K,5,RTRU,45,RPME
47. K,6,RTRU,45,1
48. KMOVE,6,11,RTRU,45,999,1,RPIP,999,999
49. L,1,5,12
50. L,5,2,12
51. L,4,6,12
52. L,6,3,12
53. L,5,6,4,0.3
54. TYPE,1
55. REAL,2
56. A,1,5,6,3
57. A,5,2,4,6
58. AMESH,ALL
59. CSYS,1
60. K,7,RPIP,90,MECE
61. K,8,RPIP,THED,MECE
62. K,9,RPIP,THED

63. K,10,RPIP,-90,
64. K,11,RPIP,-90,MECE
65. K,12,RPIP,-90,LORT
66. K,13,RPIP,THED,LORT
67. K,14,RPIP,90,LORT
68. K,15,RPIP,MIDD
69. K,16,RPIP,MIDD,MECE
70. K,17,RPIP,MIDD,LORT
71. L,3,9,12,1.5
72. L,6,8,12,1.5
73. L,4,7,12,1.5
74. REAL,1
75. TYPE,1
76. L,8,9,12
77. L,7,8,12
78. A,3,6,8,9
79. A,6,4,7,8
80. TYPE,1
81. L,8,16,6
82. L,16,15,12
83. L,15,9,6
85. L,16,11,6
86. L,11,10,12
87. L,10,15,6
88. A,9,8,16,15
89. A,15,16,11,10
90. L,7,14,16
91. L,14,13,12
92. L,13,8,16
93. A,8,7,14,13
94. L,13,17,6
95. L,17,16,16

96. A,8,13,17,16
97. L,17,12,6
98. L,12,11,16
99. A,16,17,12,11
100. AMESH,ALL
101. CSYS,0
102. SYMBC,0,1,0,0.005
103. SYMBC,0,3,0,0.005
104. MERGE,0.001
105. NALL
106. EALL
107. F,6,FY,PLB2,,16,1
108. F,70,FY,PLB2,,80,1
109. F,4,FY,PLB1
110. F,69,FY,PLB1
111. F,5,FY,PLB2
112. NSEL,Z,LORT
113. D,ALL,ALL
114. NALL
115. EALL
116. /VIEW,,1,1,1
117. KNUM,1
118. KPLOT
119. /VIEW,,1,1,1
120. WFRONT
121. WSTART,ALL
122. WAVES
123. APLOT,ALL
124. /PBC,FORCE,1
125. /PBC,TDIS,1
126. /PBC,RDIS,
127. /PBC,PRES,1

```
NPLOT
EPLOT
ITER,1,1,1
AFWRITE,,1
FINISH
/EXEC
/INPUT,27
FINISH
/POST1
/OUTPUT,35
/TITLE CASE-1   1/4  MODEL CIRCUMFERENTIAL  DIRECTION
/COM RADIAL FORCE
/COM BETA=0.30  GAMMA=10  t=BETA*T  P=-1000
/AUTO
STORE,STRES,DISP
/NOPR
/NOLIST
STRESS,SXCT,63,9
STRESS,SYCT,63,10
STRESS,SXYT,63,11
STRESS,SXCM,63,13
STRESS,SYCM,63,14
STRESS,SXYM,63,15
STRESS,MXC,63,6
STRESS,MYC,63,7
STRESS,MXYC,63,8
STRESS,NXIT,63,21
STRESS,NYIT,63,22
STRESS,NXIM,63,37
STRESS,NYIM,63,38
STRESS,PXCT,63,129
STRESS,PYCT,63,130
```

160. STRESS,PZCT,63,131
161. STRESS,PSIT,63,132
162. STRESS,SGET,63,133
163. STRESS,PXCM,63,134
164. STRESS,PYCM,63,135
165. STRESS,PZCM,63,136
166. STRESS,PSIM,63,137
167. STRESS,SGEM,63,138
168. STRESS,PSST,63,151
169. STRESS,PSSB,63,152
170. SET
171. NSEL,NODE,81
172. ENODE
173. NASEL,NODE,21
174. ENODE
175. PRELEM
176. PRSTRS,SXCT,SYCT,SXYT,SZCT,NXIT,NYIT,PXCT,PYCT,PZCT,PSIT
177. PRSTRS,SXCM,SYCM,SXYM,SZCM,NXIM,NYIM,PXCM,PYCM,PZC
178. M,PSIM
179. PRSTRS,MXC,MYC,MXYC,PSST,PSSB,SEGT,SEGM
180. NELEM
181. TOP
182. PRNSTR,ALL
183. MID
184. PRNSTR,ALL
185. NASEL,NODE,22,32,1
186. NASEL,NODE,81,95,1
187. NASEL,NODE,17
188. ENODE
189. NSORT,SY,,,6
190. TOP
191. PRNSTR,ALL

192. MID
193. PRNSTR,ALL
194. NUSORT
195. ESORT,SYCT,,,20
196. PRSTRS,SXCT,SYCT,SXYT,SZCT,NXIT,NYIT,PXCT,PYCT,PZCT,PSIT
197. PRSTRS,SXCM,SYCM,SXYM,SZCM,NXIM,NYIM,PXCM,PYCM,PZC
198. M,PSIM
199. PRSTRS,MXC,MYC,MXYC,PSST,PSSB,SEGT,SEGM
200. NUSORT
201. NSORT,DISP,,,10
202. PRDISP
203. AVPRIN
204. PRNSTR,ALL
205. NALL
206. EALL
207. /VIEW,,1,1,1
208. PLNSTR,SIGE,SZ
209. PLNSTR,SIGE,SX
210. PLNSTR,SX
211. PLNSTR,SY
212. SET,1,1
213. SAVE
214. FINISH

APPENDIX D. PROGRAM FOR CALCULATION OF STRESS ON THE PIPE

```
#include<stdio.h>
#include<math.h>
#include<stdlib.h>
/*.Calculation of the stresses on Bending(S1,S2),Membrane(S3,S4)..*/
main( )
{
double,gama,beta,thnz,thnp,Vc,Rm,A,B, SXCT,SYCT,SXYT,SXCM,SYCM,SXYM,Mx,Mf,Nx,Nf,Nfx,S1,S2,S3,S4;
{
scanf("%lf %lf %lf %lf %lf %lf",&gama,&beta,&SXCT,&SYCT,&SXCM,& SYCM);
thnp=0.2;
Vc=1000;
thnz=beta*thnp;
Rm=gama*thnp;
A=Vc/(Rm*thnp);
B=6*Vc/(thnp*thnp);
Mx=SXCT-SXCM;
Mf=SYCT-SYCM;
Nx=SXCM;
Nf=SYCM;
S1=Mx/B;
S2=Mf/B;
S3=Nf/A;
S4=Nx/A;
 printf("%s %s %s %s %s %s\n","beta","S1","S2","S3","S4","gama");
 printf("%3.2f %8.6f %8.6f %8.6f %8.6f %3.2f\n",beta,S1,S2,S3,S4,gama);
}
}
```

APPENDIX E.PROGRAM FOR CALCULATION OF STRESS ON THE NOZZLE

```
#include<stdio.h>
#include<math.h>
#include<stdlib.h>
/*.Calculation of the stresses on Bending(S1,S2),Membrane(S3,S4)..*/
main( )
{
double,gama,beta,thnz,thnp,Vc,Rm,A,B, SXCT,SYCT,SXYT,SXCM,SYCM,SXYM,Mx,Mf,Nx,Nf,Nfx,S1,S2,S3,S4;
{
scanf("%lf %lf %lf %lf %lf %lf",&gama,&beta,&SXCT,&SYCT,&SXCM,&SYCM);
Vc=1000;
thnp=0.2;
thnz=beta*thnp;
Rm=gama*thnp;
A=Vc/(Rm*beta*thnz);
B=6*Vc/(thnz*thnz);
Mx=SXCT-SXCM;
Mf=SYCT-SYCM;
Nx=SXCM;
Nf=SYCM;
S1=Mx/B;
S2=Mf/B;
S3=Nf/A;
S4=Nx/A;
 printf("%s %s %s %s %s %s\n","beta","S1","S2","S3","S4","gama,");
printf("%3.2f %8.6f %8.6f %8.6f %8.6f %3.2f\n",beta,S1,S2,S3,S4,gama);
}
}
```

BIBLIOGRAPHY

1. Bijlarrd, P. P. " Stresses from Local Loading in Cylindrical Pressure Vessels." *Trans ASME 77,* 1955.

2. Wichman, K. R. , A. G. Hopper and J. L. Mershon, " Local Stresses in Spherical and Cylindrical Shells Due to External Loading." *Welding Research Council Bulltin No. 107,*1965.

3. Gwalteny, R. C., Corum, J. M., Balt, S. E., and Bryson, J. W., " Experimental Stress Analysis of Cylinder-to cylinder Shell Models and Comparison with Theoretical Predictions. " *Trans ASME 76,*1976.

4. Brown, S. J., Jr., Haizlip, L.D., Nielsen, J. M., Reed, S. E., " Analytical and Experimental Stress Analysis of a Cylinder-to cylinder Structure." *ASME, Journal of Pressure Vessel Tech., November,* 1977.

5. Sadd, M. H. Avent, R. R., "Stress Analysis and Stress Index Development for a Trunnion Pipe Support." *ASME, Journal of Pressure Vessel Technology, Vol. 104,* 1982.

6. Tabone, C. J. mallett, R. H., " Pressure-plus-moment limit-locd Analysis for a Cylindrical Shell Nozzle." *ASME, journal of Pressure Vessel Tech. Vol.109,* 1987.

7. Mirza, S., Gupgupogl, K., " Stress Analysis of Pressure Vessels with Uniformly Spaced Lugs." *Tran of ASME, Vol.110,* 1968.

8. J. C. Sun, B. C. Sun and H. Herman , " Finite Element Analysis of Piping-nozzle Connections. Part II-localized, " *Proceeding, PUP-Vol. 194, ASME, PUPD Conference.Nashville, Tenn,*1990.

9. H. C. Sun, "On Local Stresses and Spring Constants of Pipe-nozzle Connection." *Doctor Dissertation, NJIT, Newark, NJ,*1990.

10. Timoshenko, S., Woinowsky, krieger, S., Theory of Plates and Shells, *Second Edition, McGraw-Hill, Inc.* 1959.

11. ANSYS 4.0, *Swanson Analysis Systems Inc.* 1989.

12. Tempgraph 2.4, *Mihalisin Associates Inc.* 1991.

13. FrameMaker Version 3.0 *Frame Technology Corporation.*